Analytica Chimica Acta 902 (2016) 50–58

Contents lists available at ScienceDirect

Analytica Chimica Acta

journal homepage: www.elsevier.com/locate/aca

Enhanced fluorescence sensitivity by coupling yttrium-analyte complexes and three-way fast high-performance liquid chromatography data modeling

Mirta R. Alcaraz, María J. Culzoni**, Héctor C. Goicoechea*

Laboratorio de Desarrollo Analítico y Quimiometría (LADAQ), Cátedra de Química Analítica I, Facultad de Bioquímica y Ciencias Biológicas, Universidad Nacional del Litoral-CONICET, Ciudad Universitaria, 3000, Santa Fe, Argentina

HIGHLIGHTS

- Highly sensitive method for the analysis of seven fluoroquinolones.
- Coupling of yttrium-analyte complex and three-way modeling.
- Complex or tedious sample treatments or enrichment processes are nor required.
- Accuracy on the quantitation of fluoroquinolones in real water river samples.

GRAPHICAL ABSTRACT

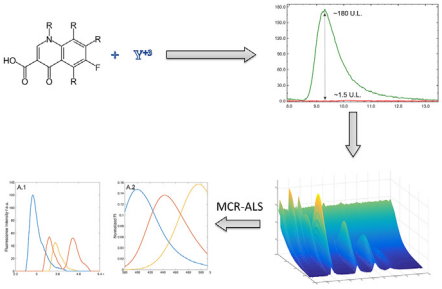

ARTICLE INFO

Article history:
Received 14 August 2015
Received in revised form 22 October 2015
Accepted 26 October 2015
Available online 17 November 2015

Keywords:
Fluoroquinolones
HPLC-FSFD
Emerging contaminants
Second-order data

ABSTRACT

The present study reports a sensitive chromatographic method for the analysis of seven fluoroquinolones (FQs) in environmental water samples, by coupling yttrium-analyte complex and three-way chromatographic data modeling. This method based on the use of HPLC-FSFD does not require complex or tedious sample treatments or enrichment processes before the analysis, due to the significant fluorescence increments of the analytes reached by the presence of Y^{3+}. Enhancement achieved for the FQs signals obtained after Y^{3+} addition reaches 103- to 1743-fold. Prediction results corresponding to the application of MCR-ALS to the validation set showed relative error of prediction (REP%) values below 10% in all cases. A recovery study that includes the simultaneous determination of the seven FQs in three different environmental aqueous matrices was conducted. The recovery studies assert the efficiency and the accuracy of the proposed method. The LOD values calculated are in the order of part per trillion (below 0.5 ng mL^{-1} for all the FQs, except for enoxacin). It is noteworthy to mention that the method herein proposed, which does not include pre-concentration steps, allows reaching LOD values in the same order of magnitude than those achieved by more sophisticated methods based on SPE and UHPLC-MS/MS.

1. Introduction

The imminent increase of research activities concerning environmental issues is mainly related to the frequent occurrence of new pharmaceuticals, both veterinary and human, in several environmental sources, i.e., surface water, groundwater, wastewater

* Corresponding author.
** Corresponding author.
E-mail addresses: mculzoni@fbcb.unl.edu.ar (M.J. Culzoni), hgoico@fbcb.unl.edu.ar (H.C. Goicoechea).

http://dx.doi.org/10.1016/j.aca.2015.10.038
0003-2670/

and even drinking water [1,2]. Evaluation and monitoring of traces of these so-called "emerging" contaminant are imperative for human health protection as well as environmental control [2]. Therefore, sensitive, fast, and simple analytical methods are demanded. Over the last years, analytical methods based on fluorometric techniques have attracted considerable attention due to their ability to combine the three characteristics aforementioned.

By virtue of their selectivity and sensitivity, luminescent probes have demonstrated to be a good alternative to measure different compounds in diverse matrices. Metal ions, especially rare-earth ions, such as Terbium (Tb^{3+}) and Europium (Eu^{3+}) [3–5], as well as metal nanoparticles [6,7] are usually used as luminescent probes due to their singular luminescence characteristics: 1 – narrow spectral width, 2 – long luminescence life-time, 3 – large Stokes shift, and 4 – strong combination ability [8,9]. Recently, it has been demonstrated that Yttrium (Y^{3+}), a non-lanthanide element, could remarkably enhance the native fluorescence of several fluoroquinolones [9–13]. Y^{3+} in solution does not have native fluorescence by itself, but in presence of certain pharmaceuticals, i.e., fluoroquinolones (FQs), is able to enhance the native fluorescence of the analytes [9–11]. These Y^{3+} based systems for the analysis of pharmaceuticals would not require complicated or tedious treatment procedure (sample clean-up or pre-concentration steps) to achieve lower limits of detection, due to the fact that the increment of the native fluorescent of the analytes is giving in a quasi-selective way. Here, FQ reacts as a bidentate ligand to the Y^{3+} through the pyridine oxygen and carboxylate oxygen forming a strong and stable complex [10,14], leading both an increase of native fluoresce intensity as a change in the maximum wavelength position [11].

In the 1980s, FQs were developed as an effective group of antibiotics for the treatment of bacterial infections in humans, animals, poultry, and fish [15]. Since these compounds are not fully metabolized by the body and are not fully removed in wastewater treatment plants, they are discharged into surface water supplies as parent compound or as sub-product of the parent compound [16]. Besides, considering they are administrated in large quantities and do have high resistance to biodegradation, these compounds are of public and ecological health concern [15,16], mainly because is not well-known the health effect if they persist in the environment even at very low levels [17]. Hereof, simple and fast analytical methods capable of measuring trace concentrations of fluoroquinolones in several aqueous matrices are required.

A large number of methods for the determination of FQs in environmental water samples could be found in the literature, including chromatographic methods with fast-scanning fluorescence (FSFD) detection, mass spectrometry detection (MS) or diode-array detection (DAD), obtaining second-order data [18]. Recently, a high-performance liquid chromatographic (HPLC) method coupled to fluorescence detection, recording excitation-emission matrices as a function of elution time generating third-order data, has been published [19,20]. Also, a recent report proposes a method for quantitation of FQs in drinking water using capillary electrophoresis with DAD [21]. In this regard, multivariate calibrations can be implemented to model these data achieving considerable improvement in analytical properties [18] as well as a decrease of costs and time of analysis, contributing to the green analytical chemistry principles [22].

Due to the low concentration of FQs found in environmental waters and the complexity of these matrices, suitable sample pretreatments and enrichment processes are crucial steps in these analyses. It has been demonstrate that solid-phase extraction (SPE) is the technique most widely used both as pre-concentration processes as a technique to remove matrix effects associated with the composition of the sample [16]. Nevertheless, several enrichment techniques have been reported with the aim to reach increasingly low limits of FQs is several environmental matrices, e.g., ultrasound-assisted ionic liquid dispersive liquid–liquid microextraction (DLLME) [23] and salting-out assisted liquid–liquid extraction (SALLE) [1], but increasing the complexity of the entire procedure with an increase of costs and time of analysis.

The present study reports a sensitive chromatographic method for the analysis of seven fluoroquinolones, including enoxacin, ofloxacin, norfloxacin, ciprofloxacin, enrofloxacin, sarafloxacin, and difloxacin, in environmental water samples, by coupling yttrium-analyte complex and three-way chromatographic data modeling. This method based on the use of HPLC-FSFD does not require complex or tedious sample treatments or enrichment processes before the analysis, due to the significant fluorescence increments of the analytes reached by the presence of Y^{3+}.

With the purpose of evaluating the application of the method to environmental water samples, determination of FQs in surface water, well water and wastewater was carried out.

2. Experimental section

2.1. Chemicals and reagents

All standards were of analytical grade. Enoxacin (ENO), norfloxacin (NRF), ofloxacin (OFL) and sarafloxacin (SRF) were provided by Sigma–Aldrich (Steinheim, Germany). Ciprofloxacin (CPF), difloxacin (DIF) and enrofloxacin (ENF) were purchased from Fluka (Buchs, Switzerland). Acetonitrile (ACN) LC grade was obtained from LiChrosolv (Merk Millipore Co., Darmstadt, Germany). Ultrapure water was obtained from a Milli-Q purification system from Millipore (Bedford, USA). Glacial acetic acid (HAc) was purchased from Merk (Darmstadt, Germany) and sodium acetate trihydrate (NaAc) was provided by Anedra (La Plata, Argentina). Yttrium (III) nitrate hexahydrate ($Y(NO_3)_3{\cdot}6H_2O$) was purchased from Sigma–Aldrich (Steinheim, Germany).

Stock standard solutions of each FQ were prepared by dissolving the appropriate amount of each FQ in alkalinized methanol (pH 9.00) to reach concentration levels of 200.00 $\mu g\ mL^{-1}$, and stored at 4 °C in the dark.

A stock standard solution of yttrium (Y^{3+}) was prepared by dissolving the appropriate amount of $Y(NO_3)_3{\cdot}6H_2O$ in ultrapure water in order to obtain a concentration of 0.1 mol L^{-1}.

A 0.02 mol L^{-1} acetic acid/acetate buffer solution (AcYB) was prepared by dissolving the appropriate amount of NaAc in ultrapure water, and adjusting the pH to 4.00 with glacial HAc. The solution was transferred to a 1000.00 mL volumetric flask and 1.00 mL of the standard solution of Y^{3+} was added in order to obtain an Y^{3+} final concentration of 1.0×10^{-4} mol L^{-1}. Then, the volume was completed to the mark with ultrapure water.

2.2. Instrumentation and procedure

The experiments were performed on an Agilent 1100 LC instrument (Agilent Technologies, Waldbronn, Germany), equipped with degasser, quaternary pump, auto-sampler, oven column compartment, UV–Vis Diode Array Detector (DAD), fast-scanning fluorescence detector (FSFD) and ChemStation software package (Agilent Technologies, Waldbronn, Germany) to control the instrument, the data acquisition and the data analysis.

The separation was performed on a 3.5 μm Zorbax Eclipse XDB-C18 analytical column (75 mm × 4.6 mm) (Agilent Technologies, Waldbronn, Germany) in isocratic mode at 2.20 mL min^{-1} flow rate during 16.0 min at 45 °C. The mobile phase consisted in a mixture of AcYB and ACN (91:9).

All pH measurements were carried out with an Orion (Massachusetts, United States) 410A potentiometer equipped with a Boeco BA 17 (Hamburg, Germany) combined glass electrode.

2.3. Data generation and software

The time-emission fluorescence data matrices (TEM) were registered in the emission spectral range between 380.0 nm and 510.0 nm, with the excitation wavelength fixed at 280.0 nm, in the elution time ranged from 0.0 to 16.0 min. The detector gain was set at 18, and the scan speed was 180 nm s^{-1}. In this way, TEM consisted in 1012 × 132 data points for elution time and spectral dimension, respectively.

Data processing and MCR-ALS analysis was performed in MATLAB 7.10 [24]. MCR-ALS algorithms are available online at http://www.mcrals.info/.

2.4. Calibration and validation samples

A calibration set of five pure standard samples for each FQ was daily prepared in triplicate by transferring appropriate aliquots of each FQ stock solution and 5.0 μL of Y^{3+} solution to 5.00 mL volumetric flasks and completing to the mark with ultrapure water. The final concentrations were ranged between 0.00 and 30.00 ng mL^{-1} for CPF, ENF and NRF; 0.00 and 200.00 ng mL^{-1} for ENO; 0.00 and 90.00 ng mL^{-1} for DIF; 0.00 and 36.00 ng mL^{-1} for OFL and 0.00 and 84.00 ng mL^{-1} for SRF. The final concentration for Y^{3+} was 1.0 × 10^{-4} mol L^{-1}. Considering that NRF and CPF, as well as SRF and DIF, present identical emission spectra and quasi-complete chromatographic resolution, they were calibrated as follows: a mixed solution containing NRF and CPF was prepared in triplicate by transferring appropriate aliquots of NRF and CPF stock solution and 5.0 μL of Y^{3+} solution to 5.00 mL volumetric flasks and completing to the mark with ultrapure water. The same procedure was followed for the simultaneous calibration of SRF and DIF.

An eleven-sample validation set was built considering FQ concentrations different than those used for calibration, and following a random design detailed in Table 1. The validation samples were prepared as previously described for the calibration samples.

Validation and calibration samples were filtered using 0.45 μm pore size nylon membranes (MSI, Osmonics Inc, Minnesota, United States) and transferred to 2 mL vials. Finally, 100 μL were injected into the chromatographic system.

2.5. Environmental water samples

Water samples obtained from three different sources were analyzed. Surface water was gathered from Las Prusianas stream (Santa Fe, Argentina), wastewater was collected from different effluents of Facultad de Bioquímica y Ciencias Biológicas (Santa Fe, Argentina) and well water was obtained from Colastiné city (Santa Fe, Argentina). All samples were collected in 1 L amber bottles with Teflon-lined caps, and processed immediately after arrival to the laboratory or stored at 4 °C until all assays were performed. Before injection into the chromatographic system, the samples were centrifuged at 4000 rpm for 10 min and filtered through 0.45 μm pore size nylon membranes.

Three sets of twelve water samples including blank samples and spiked samples with three concentration levels of each FQ were analyzed in triplicate. Spiked samples were prepared following the procedure mentioned for the calibration samples, but completing the volume flasks to the mark with each water sample instead of ultrapure water. Spiked concentrations of each FQ in these samples are summarized in Table 2.

Table 1
Prediction results on validation samples using MCR-ALS.[a]

Validation sample	ENO		NRF		OFL		CPF		ENF		SRF		DIF	
	Nominal	Predicted	Nominal	Predicted	Nominal	Predicted	Nominal	Predicted	Nominal	Predicted	Nominal	Predicted	Nominal	Predicted
M01	125.0	119.5	15.0	13.6	30.0	33.2	25.0	25.7	15.0	13.7	24.0	24.6	80.0	76.3
M02	175.0	159.2	5.0	5.4	6.0	5.4	5.0	4.6	25.0	22.6	48.0	48.0	40.0	40.7
M03	75.0	74.2	5.0	5.0	30.0	29.0	25.0	22.8	0.8	0.8	48.0	44.4	80.0	82.4
M04	25.0	26.1	0.8	0.6	18.0	19.8	15.0	14.2	0.8	0.7	9.0	8.5	60.0	65.2
M05	175.0	158.0	5.0	5.5	18.0	18.0	15.0	13.6	25.0	25.6	48.0	50.0	60.0	66.0
M06	125.0	115.1	15.0	14.5	18.0	17.7	15.0	14.9	15.0	13.8	24.0	25.7	60.0	64.2
M07	75.0	72.7	25.0	26.1	6.0	6.6	5.0	5.4	5.0	4.8	72.0	77.7	60.0	57.9
M08	25.0	26.2	5.0	5.4	6.0	6.1	5.0	4.5	0.8	0.8	9.0	9.4	40.0	40.9
M09	175.0	162.4	5.0	5.3	6.0	5.5	5.0	4.5	25.0	22.8	48.0	47.6	40.0	40.8
M10	125.0	130.2	15.0	15.9	0.8	0.8	0.8	0.8	15.0	13.8	24.0	25.0	20.0	21.3
M11	75.0	72.7	25.0	26.0	0.8	0.8	0.8	0.8	5.0	5.4	72.0	79.0	40.0	40.2
RMSE[b]	8.88		0.74		1.19		0.89		1.20		3.06		3.49	
REP%[c]	8.70		5.98		8.06		7.26		9.73		7.74		6.99	
Mean Recovery ($\bar{R}_{exp}$)	97.1		100.8		100.8		96.2		95.5		102.4		103.0	
Standard deviation of recoveries (SR)	5.4		10.3		7.0		6.1		6.3		5.4		4.7	
t_{exp}[d]	1.8		0.3		0.4		1.9		2.2		1.4		2.1	

[a] Concentrations are given in ng mL^{-1}.

[b] RMSE: Root mean square error, $RMSE = \sqrt{\frac{1}{I}\sum_{1}^{I}(c_{nom} - c_{pred})^2}$, where I = 11.

[c] REP: Relative error of prediction, $REP = 100 \times \frac{RMSE}{\bar{c}}$, where $\bar{c}$ is the mean calibration concentration.

[d] Experimental t_{exp} value, $t_{exp} = |100 - \bar{R}_{exp}| \frac{\sqrt{N}}{SR}$, where N = 11 is the number of validation samples. (Critical value $t_{(0.025,10)} = 2.228$).

Table 2
Recovery study for FQ in spiked environmental water samples using MCR-ALS.[a]

Sample	ENO		NRF		OFL		CPF		ENF		SRF		DIF	
	Taken	Found	Taken	Found	Taken	Found	Taken	Found	Taken	Found	Taken	Found	Taken	Found
We[c]	0.0	ND[b]	0.0	ND	0.0	ND	0.0	ND	0.0	ND	0.0	ND	0.0	ND
We_01	40.0	36.3	5.0	4.6	12.0	12.6	5.0	4.7	5.0	4.6	60.0	58.3	50.0	45.1
We_02	160.0	145.5	25.0	23.1	36.0	38.0	10.0	10.4	10.0	9.2	12.0	11.8	25.0	22.9
We_03	100.0	92.8	10.0	10.3	36.0	35.3	25.0	24.6	25.0	22.8	36.0	36.7	50.0	54.9
Wa[d]	0.0	ND	0.0	ND	0.0	ND	0.0	ND	0.0	ND	0.0	ND	0.0	ND
Wa_01	40.0	37.8	5.0	4.7	12.0	13.1	5.0	4.9	5.0	4.6	60.0	55.1	50.0	46.0
Wa_02	160.0	159.4	25.0	23.0	36.0	34.1	10.0	10.7	10.0	10.9	12.0	11.8	25.0	23.5
Wa_03	100.0	107.9	10.0	10.8	36.0	36.4	25.0	25.2	25.0	25.4	36.0	32.6	50.0	51.0
SP[e]	0.0	ND	0.0	1.0	0.0	ND	0.0	0.4	0.0	3.6	0.0	ND	0.0	ND
SP_01	40.0	43.6	5.0	5.4[f]	12.0	12.9	5.0	4.7[f]	5.0	5.3[f]	60.0	55.5	50.0	50.0
SP_02	160.0	159.4	25.0	23.9[f]	36.0	35.0	10.0	10.8[f]	10.0	10.8[f]	12.0	12.4	25.0	26.7
SP_03	100.0	103.3	10.0	10.1[f]	36.0	38.9	25.0	22.9[f]	25.0	24.7[f]	36.0	34.4	50.0	50.1
Mean Recovery ($\overline{R}_{exp}$)	98.7		98.4		102.9		99.5		99.0		96.6		98.5	
Standard deviation of recoveries (SR)	7.0		6.7		5.3		5.9		7.5		4.4		7.0	
t_{exp}[g]	0.5		0.7		1.6		0.2		0.4		2.2		0.6	

[a] Concentrations are given in ng mL^{-1}. Each mean value is the average of three replicates, and recoveries (between parentheses) are given in percentage.
[b] ND, not detected.
[c] We, well water from Colastiné City (Santa Fe, Argentina).
[d] Wa, wastewater from Facultad de Bioquímica y Ciencias Biológicas (Santa Fe, Argentina).
[e] SP, Las Prusianas stream (Santa Fe, Argentina).
[f] Difference between concentration found in spiked sample and blank sample.
[g] Experimental t_{exp} value, $t_{exp} = |100 - \overline{R}_{exp}| \frac{\sqrt{N}}{S_R}$, where N = 9 is the number of environmental water samples. (Critical value $t_{(0.025,8)} = 2.306$).

3. Results and discussion

3.1. Optimization of the yttrium concentration

The fluorescence intensity enhancement promoted by the addition of Y^{3+} has been verified for all the studied FQs. The results show that the fluorescence intensity depends on the metal concentration. When the Y^{3+} concentration is lower than 1×10^{-4} mol L^{-1} the fluorescence intensity significantly increases reaching a maximum value, and remaining constant with increasing the metal concentration. Thenceforth, the Y^{3+} concentration was fixed at 1×10^{-4} mol L^{-1} for all experiments. In these conditions, the mole ratio of yttrium to FQs at final solution was 1000:1 (Y^{3+}:FQs; considering the highest concentration of the FQs), ensuring the excess of Y^{3+} over the experiments.

An evidence of the Y^{3+} effect can be appreciated in Fig. 1, in which the imperceptible native fluorescence for a solution having 60.00 ng mL^{-1} of SRF in the absence of Y^{3+} undergoes a 460-fold signal raise in the presence of the metal. Although the inset shows a slight baseline perturbation due to the presence of SRF without Y^{3+}, it is not suitable for accurate SRF quantitation. Table 3 summarized the 103- to 1743-fold signal enhancement achieved for the FQs after Y^{3+} addition. In most cases, the fluorescence increments are of considerable proportions, and, in consequence, limit of detection and quantitation extremely low, comparable to those attained by sophisticated detection methods or tedious methodology based on pre-concentration steps, are expected to be reached.

3.2. Selection of the chromatographic conditions

Some reproducibility issues related to the interaction between the FQs and Y^{3+} have been found during the development of the chromatographic method. In the first place, the inclusion of Y^{3+} solely as a component of the mobile phase caused a significant

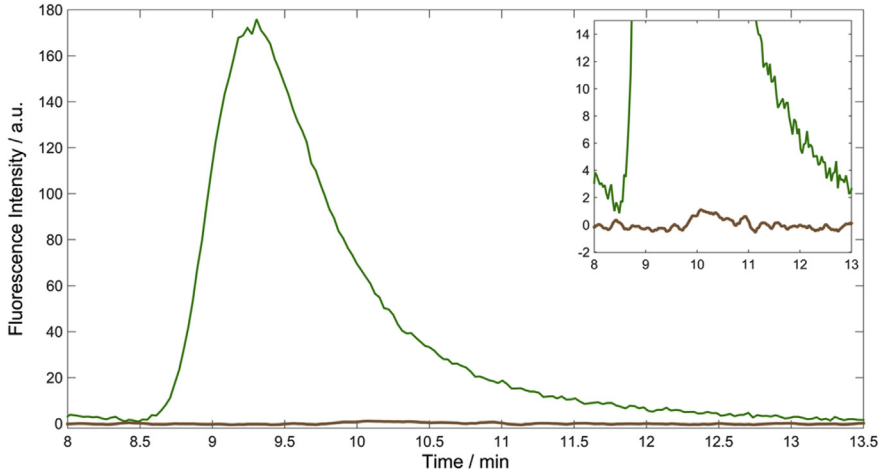

Fig. 1. Chromatograms of a 60 ng mL^{-1} SRF solution in the presence (green) and the absence (brown) of Y^{3+}. The inset shows a selected range displaying the slight signal of SRF in the absence of Y^{3+}. FSFD detection: λ_{ex} = 280.0 nm and λ_{em} = 450.0 nm. (For interpretation of the references to color in this figure legend, the reader is referred to the web version of this article.)

Table 3
Fluorescence intensity enhancement values for each FQ.

Analyte[a]	Area without Y^{3+} [b]	Area with Y^{3+} [c]	Intensity enhancement[d]
ENO	ND	424.5	>424
NRF	5.5	2918.1	531
OFL	11.3	1895.4	168
CPF	17.7	1825.6	103
ENF	8.3	1340.5	162
SRF	27.6	12690.1	460
DIF	1.5	2614.5	1743

[a] 10 ng mL^{-1} for CPF, ENF and NRF; 12 ng mL^{-1} for OFL; 50 ng mL^{-1} for ENO and DIF; and 60 ng mL^{-1} for SRF.
[b] Area obtained by liquid chromatography for each FQ without Y^{3+}. FSFD detection: λ_{ex} = 280.0 nm and λ_{em} = 450.0 nm for CPF, NRF, ENF, SRF and DIF; λ_{em} = 400.0 nm for ENO and λ_{em} = 490.0 nm for OFL.
[c] Area obtained by liquid chromatography for each FQ with Y^{3+}. FSFD detection: λ_{ex} = 280.0 nm and λ_{em} = 450.0 nm for CPF, NRF, ENF, SRF and DIF; λ_{em} = 400.0 nm for ENO and λ_{em} = 490.0 nm for OFL.
[d] Ratio between the area with Y^{3+} and the area without Y^{3+} for each FQ.

variability both in the retention times and the peak areas gathered for replicate injections of the same sample, suggesting lack of reproducibility in the complex formation from run to run. This drawback was overcome by generating the complex in the sample preparation step through the addition of Y^{3+} to the sample at the same concentration level that found in the mobile phase. The strategy was conducted under the hypothesis that the interaction between the FQs and the stationary phase precludes the complete formation of the complexes, but the presence of Y^{3+} in the mobile phase favors the stabilization of the pre-generated complex inside the column. Secondly, the percentage of organic solvent included in the mobile phase was minimized in order to benefit the complex formation, in spite of causing a slight detriment in the peak shape of some FQs, and develop a high-performance method within the framework of green analytical chemistry [8,25]. Finally, the pH of the mobile phase was selected considering the nature of the stationary phase and the interaction with FQs, as well the interaction between the FQs and Y^{3+}.

3.3. MCR-ALS performing

MCR-ALS performs a bilinear decomposition of the data matrix **D** into three matrices according to the equation 1

$$\mathbf{D} = \mathbf{C}\mathbf{S}^{T} + \mathbf{E} \quad (1)$$

where **C** is the matrix of the resolved elution time profiles, **S** contains the spectral profiles and **E** contains the residuals. Each dyad $\mathbf{c}_i\mathbf{s}_i^T$ represents the individual contribution of a component to the overall measured signal **D** [26]. With the aim to reduce ambiguities and rank deficiency problems an augmented data matrix, $\mathbf{D}_{aug}$, is building and a unique resolution is obtained for several data matrices simultaneously [27].

In case of highly complex analytical data, preprocessing procedures including both removal of chromatogram baseline and data smoothing help data analysis and improve the quality of the analytical results. With this purpose, Savitzky–Golay [28] was applied to perform an appropriate smoothing in the elution time dimension. The background correction was performed by subtracting to each chromatogram its own chromatographic baseline. A chromatographic region where no analytical signal in the whole spectral range is present, e.g. at the end of the chromatographic run, was chosen as the baseline spectral vector. Then, the baseline spectral vector was subtracted to each time of the TEM.

Under the described experimental conditions, there are two groups of analytes with identical emission spectra, i.e. NRF, CPF, and ENF, and SRF and DIF. Consequently, the resolved chromatogram exhibits spectrally rank-deficient components [25]. Since extended-MCR-ALS performed by matrix augmentation of full matrices in the elution time mode could not overcome this drawback, a simple strategy has been proposed in order to circumvent this rank-deficiency problem.

Before MCR-ALS processing, the chromatographic data were split into two regions; the first one (A) including ENO, NRF, OFL and CPF (between 2.2 and 5.4 min), and the other (B) comprising ENF, SRF and DIF (between 6.0 and 14.8), as shown in Fig. 2. However, there were still two pairs of analytes that present identical emission spectra in each region and quasi-complete chromatographic resolution. This drawback was overcome by considering each pair as if they were a single analyte while performing MCR-ALS, but with two chromatographic peaks. Afterwards, the retrieved MCR-ALS elution time profiles were split to achieve individual quantitative results, both for calibrations as validation or environmental water samples. The MCR-ALS elution time profile corresponding to NRF and CPF was divided at 3.8 min to obtain NRF (before 3.8 min) and CPF (after 3.8 min) individual contributions. Same procedure was followed for SRF and DIF elution time profile, where two regions were ranged from 8.2 to 11.2 min and from 11.2 to 14 min for SRF and DIF contribution, respectively. This procedure has demonstrated to be an efficient strategy in cases where compounds with spectral rank deficiency are present, and individual quantitative information is required [21]. Fig. 3 shows the profiles retrieved by MCR-ALS for one spiked environmental water sample.

Therefore, data processing comprised the building of two augmented column-wise $\mathbf{D}_{aug}$ ($\mathbf{D}_{augA}$ and $\mathbf{D}_{augB}$) data matrices containing, for each elution time region, the validation or environmental water sample data and the calibration data matrices. Before starting resolution, the determination of the number of spectrally active components in each $\mathbf{D}_{aug}$ data matrix was carried out by applying singular value decomposition (SVD). Then, in order to build the initial spectral estimation, the analysis of the purest spectra based on the SIMPLISMA methodology was carried out [29].

Eventually, with the purpose of driving the iterative procedure to chemically interpretable solutions, several mathematical constraints were applied, *i.e.* correspondence among species, non-negativity in both modes and unimodality in the elution time mode. It is important to highlight that the unimodality constraint was not applied to every components, considering the rank deficiency problem aforementioned.

3.4. Quantitative and qualitative analysis

After MCR-ALS decomposition of each **D** data matrix, the pseudo-univariate regression of area against concentration for each analyte was built with the concentration information for the calibration samples contained in **C** (the areas under the elution time profiles for each component).

Table 1 shows the prediction results corresponding to the application of MCR-ALS to the validation set. As can be seen, the Relative Error of Prediction (REP %) values are below 10% in all cases. In order to appraise whether the recoveries were not statistically different than 100%, a hypothesis test was applied. The experimental t_{exp} values were estimated following the Eq. (2),

$$t_{exp} = |100 - \bar{R}_{exp}| \frac{\sqrt{n}}{S_R} \quad (2)$$

where $\bar{R}_{exp}$ is the average experimental recovery and S_R the standard deviation of the recoveries. The recoveries are considering statistically different than 100% when t_{exp} value exceed the critical $t_{(\alpha,\upsilon)}$ value at level α, $\upsilon = n-1°$ of freedom and n samples [30]. Considering 95% confidence level, the experimental t_{exp} value for all FQs in validation samples are lower than critical value $t_{(0.025,10)}$

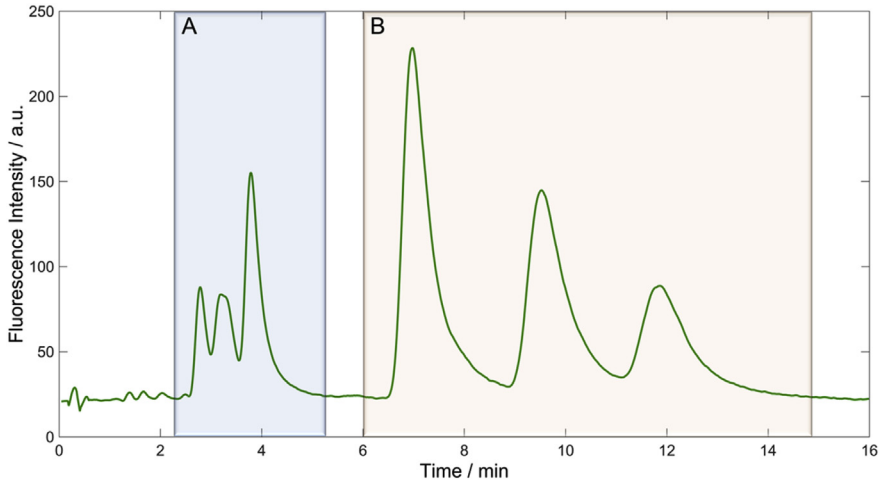

Fig. 2. Chromatogram of the validation sample M02 showing the regions generated to perform the MCR-ALS resolution: (A) includes ENO, NRF, OFL and CPF, and (B) comprises ENF, SRF and DIF. FSFD detection: λ_{ex} = 280.0 nm and λ_{em} = 450.0 nm.

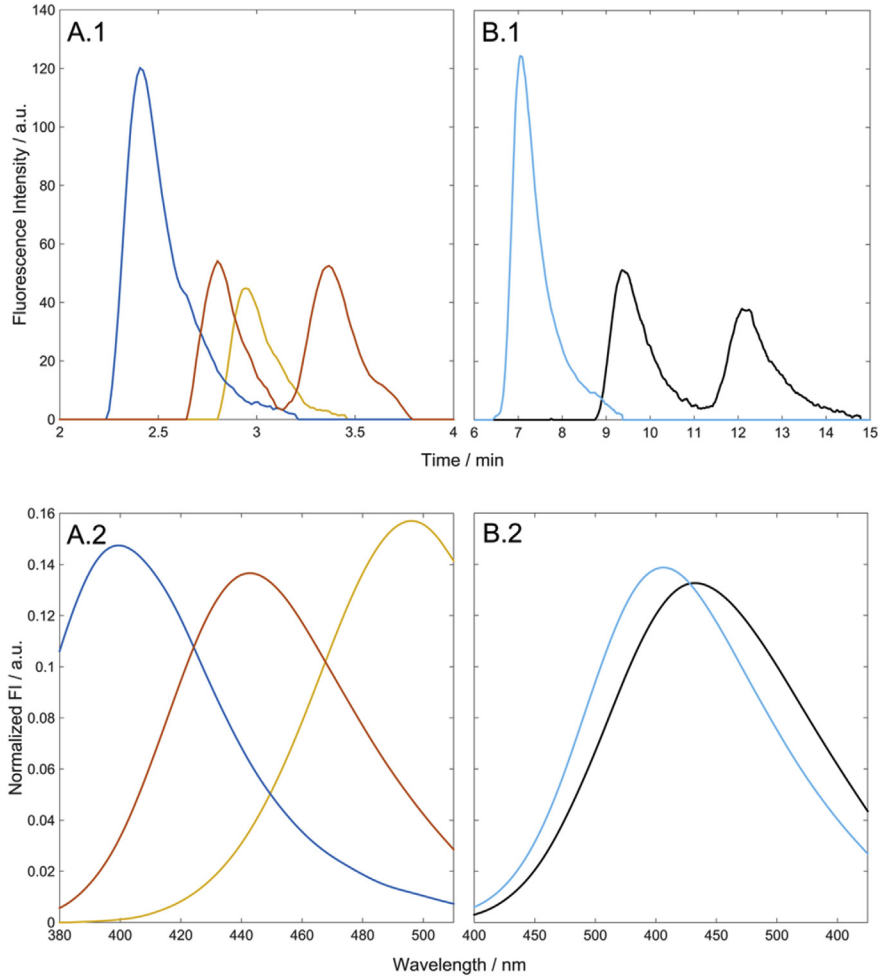

Fig. 3. Elution time and spectral profiles retrieved by MCR-ALS for spiked environmental water sample SP_01. Elution time (A.1) and spectral (A.2) profiles of ENO (blue), NRF and CPF (red), and OFL (light orange). Elution time (B.1) and spectral (B.2) profiles of ENF (light blue), and SRF and DIF (black). (For interpretation of the references to color in this figure legend, the reader is referred to the web version of this article.)

= 2.228, indicating that the recoveries are not statistically different than 100%.

As previously mentioned, a recovery study that includes the simultaneous determination of the 7 FQs in three different environmental aqueous matrices was conducted. It is worth mentioning that the samples collected at Las Prusianas stream were found to already contain NRF, CPF and ENR. Although they were all present in very low concentration, i.e. 0.4, 1.0 and 3.6 ng mL^{-1} of CPF, NRF, and ENR, respectively, the proposed method allowed their detection and quantitation avoiding sample preparation steps for clean-up and/or pre-concentration. The recovery results for the 7 FQs in three different environmental aqueous matrices are summarized in Table 2. Here, the experimental t_{exp} value for all FQs are lower than critical value $t_{(0.025,8)} = 2.306$, asserting the efficiency and the accuracy of the proposed method.

These results are indicative of the method suitability for precisely measuring the extremely low FQ concentration herein being evaluated.

In order to quantitatively evaluate the comparability of the pure spectra ($\mathbf{s}_1$) and MCR-ALS retrieved spectra ($\mathbf{s}_2$) by the degree of spectral overlap (s_{12}) the following expression was employed

$$s_{12} = \frac{\|\mathbf{s}_1^{T}\mathbf{s}_2\|}{\|\mathbf{s}_1\|\,\|\mathbf{s}_2\|} \quad (3)$$

The value of s_{12} ranges from 0 to 1, corresponding to no overlapping and complete overlapping, respectively [31].

Using equation (3), the s_{12} values obtained for ENO, NRF/CPF, OFL, ENF, and SRF/DIF were 0.9998, 0.9999, 0.9999, 0.9997, 1.000 and 0.9998, respectively. These figures allow us to conclude that the spectra retrieved by MCR-ALS are comparable to the pure spectra demonstrating a high quality modeling.

3.5. Figures of merit

In analytical chemistry, figures of merit (FOMs) are numerical parameters useful to compare the relative performances of different analytical methodologies, and also to discriminate their detection capabilities [32]. When estimating them, it is crucial to consider the calibration data order to obtain consistent numerical parameters that represent the system. Additionally, in the case of multiway data, the algorithm used to process the data should be contemplated [33].

FOMs such as limit of detection (LOD) and quantitation (LOQ) are related to the sensitivity (SEN) of a method, which is also a FOM to be estimated. When MCR-ALS is applied to second-order multivariate calibration data, SEN is assessed using the following expression [34]:

$$\mathrm{SEN}_{\mathrm{MCR}} = p_k\left[J\left(\mathbf{S}^{T}\mathbf{S}\right)^{-1}_{kk}\right]^{-1/2} \quad (4)$$

where k is the index for the analyte of interest in a multicomponent mixture, J is the number of data points in each submatrix in the augmented mode, and p_k is the slope of the MCR-ALS pseudo-univariate graph. As could be seen, SEN depends on the non-augmented profiles **S**. Then, $\mathrm{LOD}_{\mathrm{MCR}}$ and $\mathrm{LOQ}_{\mathrm{MCR}}$ are estimated following equations (5) and (6), respectively [34]:

$$\mathrm{LOD}_{\mathrm{MCR}} = 2t_{\alpha,\upsilon}s_c = \frac{2t_{\alpha,\upsilon}s_{dtest}}{\mathrm{SEN}_{MCR}} \quad (5)$$

$$\mathrm{LOQ}_{\mathrm{MCR}} = 10s_c = 10\frac{\mathrm{LOD}_{MCR}}{2t_{\alpha,\upsilon}} \quad (6)$$

for a non-central t distribution with $\upsilon = n{-}2^{\circ}$ of freedom and a probability α (=0.05). s_c and sd_{test} represent the standard deviation in the predicted analyte concentrations and the standard deviation of the estimated net signal when its true value is zero (or noise level), respectively.

An alternative approach for determining FOMs consists in using the pure response profiles retrieved by MCR for the analyte species present in a sample to estimate them as it is done in univariate calibration [35]. In this case, SEN is defined as the slope of the calibration curve obtained by plotting the relative responses against concentration of the standards and does not depend on the non-augmented profiles **S**. Then $\mathrm{LOD}_{\mathrm{UnC}}$ and $\mathrm{LOQ}_{\mathrm{UnC}}$ are calculated following the equations (5) and (6), but using s_0 instead of s_c [36,37]. Here, s_0 represents an estimate of the standard deviation of the estimated net signal when its true value is zero.

On the other hand, the signal-to-noise ratio (SNR) can be used to calculate LOD and LOQ in analytical procedures that exhibit baseline noise, i.e. chromatographic or electrophoretic methodologies. In this way, SNR is determined by comparing measured signals from samples with known low concentrations of analyte with those of blank samples. SNRs in the order of 3 and 10 are generally considered acceptable for estimating $\mathrm{LOD}_{\mathrm{SNR}}$ and $\mathrm{LOQ}_{\mathrm{SNR}}$, respectively [37].

Table 4 contains the LODs and LOQs estimated for the 7 FQs using the three aforementioned approaches. As can be seen, the higher the calibration order, the better the LOD and LOQ, since SEN increases with the number of data ways and consequently decreases both the LOD and LOQ [33]. It is important to highlight that most of the FOMs calculated following the MCR-ALS approach are coincident in order of magnitude with those achieved when applying the SNR strategy, supporting the fact that the former is able to provide realistic estimations. The slight difference observed in some cases could be attributed to the fact that the MCR-ALS strategy was applied to smoothed data, i.e. subjected to noise elimination through Savitzky–Golay [28].

As stated in Table 4, the LOD values calculated using the MCR-ALS approach are below 0.5 ng mL^{-1} for all the FQs, except for ENO. These values are comparable to those reported in the determination of the same FQs in water samples, but using an UHPLC-DAD method that requires a dispersive liquid–liquid microextraction (DLLME) pre-concentration step [38]. Similar results are also observed in a very recent work in which several FQs were determined in different aqueous matrices using salting-out assisted liquid–liquid extraction (SALLE) followed by UHPLC-FD [1]. It is noteworthy to mention that the HPLC-FSFD method herein proposed, which does not include pre-concentration steps, allows to reach LODs in the same order of magnitude than those provided by a more sophisticated method based on SPE and UHPLC-MS/MS, which was applied to the simultaneous determination of several FQs in powered milk and reached LOD values between 0.14 ng mL^{-1} and 1.80 ng mL^{-1} [39]. Besides, LODs and LOQs

Table 4
Computation of LOD and LOQ values using different approaches.[a]

Analyte	MCR-ALS[b]		Univariate calibration[c]		SNR[d]	
	LOD	LOQ	LOD	LOQ	LOD	LOQ
ENO	4.7	14.3	5.2	14.7	4.1	10.3
NRF	0.05	0.1	2.6	7.2	0.2	0.5
OFL	0.1	0.3	3.3	9.3	0.2	0.4
CPF	0.07	0.2	1.3	3.6	0.2	0.5
ENF	0.06	0.2	3.4	9.6	0.2	0.4
SRF	0.5	1.6	2.7	7.5	0.9	2.2
DIF	0.4	1.1	6.9	19.4	2.3	5.9

[a] LOD, limit of detection, and LOQ, limit of quantitation, are given in ng mL^{-1}.
[b] $\mathrm{LOD}_{\mathrm{MCR}}$ and $\mathrm{LOQ}_{\mathrm{MCR}}$ calculated according to Ref. [34].
[c] $\mathrm{LOD}_{\mathrm{UnC}}$ and $\mathrm{LOQ}_{\mathrm{UnC}}$ calculated according to Refs. [36] and [41].
[d] SNR, signal-to-noise ratio using peak-to-peak noise based on ICH Q2R1 guideline. $\mathrm{LOD}_{\mathrm{SNR}}$ and $\mathrm{LOQ}_{\mathrm{SNR}}$ calculated according to Ref. [37].

reached in the present work are lower than those reported by Cañada-Cañada et al. [40] for the determination of 8 FQs also in aqueous samples, and a method previously developed by our group using SPE and EC-DAD as well [21].

4. Conclusions

The combination of HPLC-FSFD, Y^{3+}-analyte complex and three-way data modeling allowed the successful determination of 7 FQs in different environmental water samples. The fluorescence intensity enhancement of the seven studied FQs promoted by the addition of Y^{3+} has been shown to be an efficient way to reach extremely high sensitivity, which allows for quantitation of these analytes in environmental samples.

In light of the results obtained in the present work, it can be concluded that the proposed method is highly suitable for the quantitation of seven FQs in environmental water samples in a simple, fast and efficient way, without requiring neither sophisticated nor expensive instrumentation. Also, based on several reports found in the literature [12,13], and considering that FQ acts via chelation with Y^{3+} by its specific groups (pyridine oxygen and carboxylate oxygen), it is expected that the proposed method could be extended to the detection of other FQs that have not been analyzed in the present work. Additionally, the use of a chemometric algorithm such as MCR-ALS to model second-order data allows solving mixture analysis problems, even for compounds with highly overlapped signals.

Acknowledgment

The authors are grateful to Universidad Nacional del Litoral (Projects CAI+D 2012 No. 11-11 and 11-7), CONICET (Consejo Nacional de Investigaciones Científicas y Técnicas, Project PIP 2011-455) and ANPCyT (Agencia Nacional de Promoción Científica y Tecnológica, Project PICT 2014-0346) for financial support. M.R.A. thanks CONICET for her fellowship.

References

[1] N. Arroyo-Manzanares, J.F. Huertas-Perez, M. Lombardo-Agui, L. Gamiz-Gracia, A.M. Garcia-Campana, A high-throughput method for the determination of quinolones in different matrices by ultra-high performance liquid chromatography with fluorescence detection, Anal. Methods 7 (2015) 253–259.
[2] M.R. Alcaráz, R. Brasca, M.S. Cámara, M.J. Culzoni, A.V. Schenone, C.M. Teglia, L. Vera-Candioti, H.C. Goicoechea, Multiway calibration approaches to handle problems linked to the determination of emergent contaminants in waters, in: M. Khanmohammadi (Ed.), Current Applications of Chemometrics, Nova Publisers, New York, 2015, pp. 135–154.
[3] T. Wang, C. Jiang, Spectrofluorimetric determination of lecithin using a tetracycline-europium probe, Anal. Chim. Acta 561 (2006) 204–209.
[4] L. Wang, C. Guo, Z. Chu, W. Jiang, Luminescence enhancement effect for the determination of balofloxacin with balofloxacin-europium (III)-sodium dodecylbenzene sulfonate system, J. Luminescence 129 (2009) 90–94.
[5] R.-D.R.M. Aguilar-Caballos, A. Gómez-Hens, Simultaneous determination of ciprofloxacin and tetracycline in biological fluids based on dual-lanthanide sensitised luminescence using dry reagent chemical technology, Anal. Chim. Acta 494 (2003) 55–62.
[6] G. Yánez-Jácome, M. Aguilar-Caballos, A. Gómez-Hens, Luminescent determination of quinolones in milk samples by liquid chromatography/post-column derivatization with terbium oxide nanoparticles, J. Chromatogr. A 1405 (2015) 126–132.
[7] Q. Liu, Q. Zhou, G. Jiang, Nanomaterials for analysis and monitoring of emerging chemical pollutants, Trends Anal. Chem. 58 (2015) 10–22.
[8] J.R. Lakowicz, Principles of Fluorescence Spectroscopy, Springer, New York, 2006.
[9] C. Tong, X. Zhuo, Y. Guo, Y. Fang, Synchronous fluorescence determination of ciprofloxacin in the pharmaceutical formulation and human serum based on the perturbed luminescence of rare-earth ions, J. Luminescence 130 (2010) 2100–2105.
[10] C. Tong, X. Zhuo, W. Liu, J. Wu, Synchronous fluorescence measurement of enrofloxacin in the pharmaceutical formulation and its residue in milks based on the yttrium (III)-perturbed luminescence, Talanta 82 (2010) 1858–1863.
[11] Y. Han, X. Wu, J. Yang, S. Sun, The fluorescence characteristic of the yttrium–norfloxacin system and its analytical application, J. Pharm. Biomed. Anal. 38 (2005) 528–531.
[12] X. Zhu, A. Gong, S. Yu, Fluorescence probe enhanced spectrofluorimetric method for the determination of gatifloxacin in pharmaceutical formulations and biological fluids, Spectrochim. Acta Part A Mol. Biomol. Spectrosc. 69 (2008) 478–482.
[13] A.M. El-Didamony, Fluorescence probe enhanced spectrofluorimetric method for the determination of sparfloxacin in tables and biological fluids, Luminescence 26 (2011) 112–117.
[14] S.A. Sadeek, W.H. El-Shwiniy, W.A. Zordok, A. El-Didamony, Spectrosopic, structure and antimicrobial activity of new Y(III) and Zr(IV) coprofloxacin, Spectrochim. Acta Part A Mol. Biomol. Spectrosc. 78 (2011) 854–867.
[15] P. Sukul, M. Spiteller, Fluoroquinolone antibiotics in the environment, in: G.W. Ware (Ed.), Reviews of Environmental Contamination and Toxicology, Springer, New York, 2006, pp. 131–154. 2077.
[16] K. He, L. Blaney, Systematic optimization of an SPE with HPLC-FLD method for fluoroquinolone detection in wastewater, J. Hazard. Mater. 282 (2015) 96–105.
[17] S.K. Khetan, T.j. Collins, Hunab pharmaceuticals in the aquatic environment: a challenge to green chemistry, Chem. Rev. (Washington, DC, United States) 107 (2007).
[18] G.M. Escandar, H.C. Goicoechea, A. Muñoz de la Peña, A.C. Olivieri, Second- and higher-order data generation and calibration: a tutorial, Anal. Chim. Acta 806 (2014) 8–26.
[19] M.R. Alcaráz, G. Siano, M.J. Culzoni, A. Munoz de la Pena, H.C. Goicoechea, Modeling four and three-way fast high-performance liquid chromatography with fluorescence detection data for quiatitation of fluoroquinolones in water samples, Anal. Chim. Acta 809 (2014) 37–46.
[20] M.R. Alcaráz, S. Bortolalo, H.C. Goicoechea, A.C. Olivieri, A new modeling strategy for third-order fast high-performance liquid chromatographic data with fluorescence detection. Quatitation of fluoroquinolones in water samples, Anal. Bioanal. Chem. 407 (2015) 1999–2011.
[21] M.R. Alcaráz, L. Vera Candioti, M.J. Culzoni, H.C. Goicoechea, Ultrafast quantitation of six quinolones in water samples by second-order capillary electrophoresis data modeling with multivariate curve resolution–alternating least squares, Anal. Bioanal. Chem. 406 (2014) 2571–2580.
[22] A. Gałuszka, Z. Migaszewski, J. Namieśnik, The 12 principles of green analytical chemistry and the SIGNIFICANCE mnemonic of green analytical practices, TrAC Trends Anal. Chem. 50 (2013) 78–84.
[23] M.M. Parrilla Vázquez, P. Parrilla Vázquez, M.M. Galera, M.D.G. García, Determination of eight fluoroquinolones in groundwater samples with ultrasound-assisted ionic liquid dispersive liquid–liquid microextraction prior to high-performance liquid chromatography and fluorescence detection, Anal. Chim. Acta 748 (2012) 20–27.
[24] MATLAB7.10. The MathWorks Inc Natick, Massachussets, USA, 2010.
[25] C. Tistaert, H.P. Bailey, R.C. Allen, Y.V. Heyden, S.C. Rutan, Resolution of spectrally rank-deficient multivariate curve resolution: alternating least squares components in comprehensive two-dimensional liquid chromatographic analysis, J. Chemom. 26 (2012) 474–486.
[26] R. Tauler, M. Maeder, A. de Juan, Multiset data analysis: extended multivariate curve resolution, in: S.D. Brown, R. Tauler, B. Walczak (Eds.), Comprehensive Chemometrics: Chemical and Biochemical Data Analysis, Elsevier, Oxford, 2009, pp. 473–505.
[27] R. Tauler, M. Maeder, A. de Juan, Multiset data analysis: extended multivariate curve resolution, in: S.D. Brown, R. Tauler, B. Walczak (Eds.), Comprehensive Chemometrics: Chemical and Biochemical Data Analysis, Elsevier, Oxford, 2009, pp. 473–505.
[28] A. Savitzky, M.J.E. Golay, Smoothing and differentiation of data by simplified least squares procedures, Anal. Chem. 36 (1964) 1627–1639.
[29] W. Windig, J. Guilment, Interactive self-modeling mixture analysis, Anal. Chem. 63 (1991) 1425–1432.
[30] A.C. Olivieri, Practical guidelines for reporting results in single- and multi-component analytical calibration: a tutorial, Anal. Chim. Acta 868 (2015) 10–22.
[31] M.J. Culzoni, H.C. Goicoechea, G.A. Ibañez, V.A. Lozano, N.R. Marsili, A.C. Olivieri, A.P. Pagani, Second-order advantage from kinetic.spectroscopic data matrices in the presence of extreme spectral overlapping. A multivariate curve resolution – alternating least squares approach, Anal. Chim. Acta 614 (2008) 12.
[32] A.C. Olivieri, G.M. Escandar, Chapter 6-analytical figures of merit, in: A.C. Olivieri, G.M. Escandar (Eds.), Practical Three-way Calibration, Elsevier, Boston, 2014. pp. 93–107.
[33] A.C. Olivieri, Analytical figures of merit: from univariate to multiway calibration, Chem. Rev. 114 (2014) 5358–5378.
[34] M.C. Bauza, G.A. Ibañez, R. Tauler, A.C. Olivieri, Sensitivity equation for quantitative analysis with multivariate curve resolution-alternating least-squares: theoretical and experimental approach, Anal. Chem. 84 (2012) 8697–8706.
[35] J. Saurina, C. Leal, R. Compañó, M. Granados, M.D. Prat, R. Tauler, Estimation of figures of merit using univariate statistics for quantitative second-order multivariate curve resolution, Anal. Chim. Acta 432 (2001) 241–251.
[36] C.A. Clayton, J.W. Hines, P.D. Elkins, Detection limits with specified assurance probabilities, Anal. Chem. 59 (1987) 2506–2514.
[37] ICH, Validation of analytical procedures: text and methodology Q2(R1), International Conference on Harmonization of Technical Requirements for Registration of Pharmaceuticals for Human Use, 2005.

[38] A.V. Herrera-Herrera, J. Hernández-Borges, T.M. Borges-Miquel, M.Á. Rodríguez-Delgado, Dispersive liquid–liquid microextraction combined with ultra-high performance liquid chromatography for the simultaneous determination of 25 sulfonamide and quinolone antibiotics in water samples, J. Pharm. Biomed. Anal. 75 (2013) 130–137.

[39] A.V. Herrera-Herrera, J. Hernández-Borges, M.A. Rodríguez-Delgado, M. Herrero, A. Cifuentes, Determination of quinolone residues in infant and young children powdered milk combining solid-phase extraction and ultra-performance liquid chromatography–tandem mass spectrometry, J. Chromatogr. A 1218 (2011) 7608–7614.

[40] F. Cañada-Cañada, J.A. Arancibia, G.M. Escandar, G.A. Ibañez, A. Espinosa Mansilla, A. Muñoz de la Peña, A.C. Olivieri, Second-order multivariate calibration procedures applied to high-performance liquid chromatography coupled to fast-scanning fluorescence detection for the determination of fluoroquinolones, J. Chromatogr. A 1216 (2009) 4868–4876.

[41] L.A. Currie, Detection and quantification limits: origins and historical overview, Anal. Chim. Acta 391 (1999) 127–134.